

Selected Papers

Imaging of Phosphatidylcholine Bilayers by a High-Pressure Fluorescence Technique: Detection of the Packing Difference

Hitoshi Matsuki,*[1] Masaki Goto,[2] Masataka Kusube,[3] and Nobutake Tamai[1]

[1]Department of Life System, Institute of Technology and Science, The University of Tokushima, 2-1 Minamijosanjima-cho, Tokushima 770-8506

[2]Department of Preventive Dentistry, Institute of Health Bioscience, The University of Tokushima, 3-18-15 Kuramoto-cho, Tokushima 770-8504

[3]Department of Material Science, Wakayama National College of Technology, 77 Nada, Noshima, Gobo, Wakayama 644-0023

Received August 1, 2011; E-mail: matsuki@bio.tokushima-u.ac.jp

The packing states in phosphatidylcholine (PC) bilayers under high pressure were studied from fluorescence measurements using a polarity-sensitive probe Prodan. By using the Prodan fluorescence data, three-dimensional image plots, which can visually evaluate the bilayer packing, were constructed for the C16PC bilayer. It turned out from the shape of contours in the image plot constructed by the second-derivative spectra that the Prodan molecules can be distributed into multiple sites in the bilayer and move around the head-group region depending on the phase state. Furthermore, comparing the plot to those for the C17PC and C18PC bilayers, the slight difference in hydrophobicity among the PC molecules produced a marked difference in quantity of the Prodan molecules distributed among the bilayer gel, nonbilayer gel, and liquid crystalline phases of the PC membranes. The present study shows that the imaging using Prodan is useful for the evaluation of lipid bilayer packing.

It is a well-known fact that lipid bilayers, which are basic structures of biological membranes, undergo a change of state from gel phase to liquid crystal (L_α) phase with increasing temperature, and this structural change is called a main transition. In the gel phase, the hydrophobic chains of lipid molecules in the bilayer have all *trans* conformations but about one-third of the chains convert to *gauche* conformations in the L_α phase. In response to the conformational change at the main transition, the lipid bilayers pack loosely in the L_α phase due to the disordered acyl chains while they pack tightly in the gel phase due to the ordered acyl chains. The packing change of lipid bilayers between the gel and L_α phases can be evaluated by the values of order parameter determined by NMR[1–3] and membrane fluidities evaluated by ESR.[4–6]

Fluorescence techniques have been also used to examine the packing states in lipid bilayers. They can provide information regarding microscopic environments around a probe molecule incorporated into the bilayers. There are some analytical methods of fluorescence spectra such as center of spectral mass[7] and ratio of fluorescence intensity between two phases.[8,9] These methods are premised on a large spectral difference between two phases and appropriate for the detection of the main transition. For example, studies on membrane states by generalized polarization using a hydrophobic fluorescent probe, 2-dimethylamino-6-lauroylnaphthalene (Laurdan) have been reported.[10,11] Since this probe sensitively responds to the chain melting of lipid molecules at the main transition, and the value of generalized polarization becomes indices of the miscibility between gel and L_α phases and the formation of new liquid-ordered phase for lipid bilayers, the Laurdan fluorescence is frequently used in the latest research of lipid rafts.[12,13]

On the other hand, lipid bilayers undergo various phase transitions between gel phases, those between lamellar crystal and gel phases, and those between bilayer–nonbilayer phases. The packing states of the lipid bilayer also change by these transitions, but such transitions usually show much smaller packing changes than the main transition accompanied with the large hydrophobic chain melting.[14,15] In fluorescence measurements, the hydrophobic probe residing in the bilayer-core region like Laurdan highly responds to the main transition originating from the change in the core while the response of the probe to the other transitions is significantly low. Although the hydrophilic probe is used for the detection of such transitions, its response for the main transition becomes reversely low. Accordingly, it is difficult to estimate the packing states among these phases by one probe comprehensively.

We have shown in the previous papers[16,17] that a hydrophilic probe with a similar molecular structure to Laurdan, 2-dimethylamino-6-propionylnaphthalene (Prodan), which resides in the head-group region of a lipid molecule, exhibits characteristic spectral changes at gel–gel and bilayer–nonbilayer transitions like the pretransition and bilayer interdigi-

Published on the web November 29, 2011; doi:10.1246/bcsj.20110229

tation as well as the main transition. This polarity-sensitive probe enabled us to observe multiple phase transitions by one probe, and the microscopic environments of several phosphatidylcholine (PC) bilayers have been examined from the behavior of Prodan fluorescence spectra.[9,18,19] Recently, we developed a novel analytical technique by using the second derivative of original Prodan fluorescence spectra.[20,21] The analytical technique can specify the exact location of the Prodan molecules in different phases of the bilayer and is much more informative for examinations of the bilayer packing. Furthermore, three-dimensional image plots of the bilayer packing by using the second derivative spectra are constructed for several PC bilayers.[22,23] In the present study, we are concerned with the bilayer phase behavior of three kinds of diacylphosphatidylcholines with different acyl chain lengths (C*n*PC: $n = 16$, 17, and 18) under high pressure by Prodan fluorescence. The methodology of imaging of bilayer packing by high-pressure fluorescence technique using Prodan are described, and then the difference in bilayer packing among these PCs, which is caused by a slight difference in hydrophobicity, is revealed in terms of their constructed image plots.

Experimental

Materials and Sample Preparation. Three kinds of diacylphosphatidylcholines, C16PC (1,2-dihexadecanoyl-*sn*-glycero-3-phosphocholine), C17PC (1,2-diheptadecanoyl-*sn*-glycero-3-phosphocholine), and C18PC (1,2-dioctadecanoyl-*sn*-glycero-3-phosphocholine), were purchased from Sigma-Aldrich Chemical Co. (St. Louis, MO) and/or Avanti Polar Lipids, Inc. (Alabaster, AL). They were used without further purification. The fluorescence probe, 2-dimethylamino-6-propionylnaphthalene, was obtained from Molecular Probes, Inc. (Eugene, OR). Water was distilled twice from a dilute alkaline permanganate solution.

The lipid vesicles containing Prodan were made by the Bangham's method. The sample solutions suitable for the fluorescent measurements were prepared as described previously.[20,21] The lipid concentration was 1.0 mmol kg^{-1} and the molar ratio of Prodan to the lipid was 1:500 in the whole experiments. All vesicles prepared were multilamellar, and the average diameters of the vesicles were ca. 200 nm, which was confirmed from the dynamic light scattering measurements.[22] All sample solutions were protected from light until measurement.

Fluorescence Measurements. The fluorescence spectra of Prodan under atmospheric and high pressures were measured with an F-2500 spectrophotometer (Hitachi High-Technology Corp., Tokyo, Japan), which was equipped with a high-pressure cell assembly PCI-400 (Syn Corp., Ltd., Kyoto, Japan). The detailed procedure of high-pressure measurement is described elsewhere.[16,23] The excitation wavelength was 361 nm, and the emission spectra were recorded at wavelengths from 400 to 600 nm. The second derivatives of the emission spectra were obtained by using attached software (FL-solutions) of the apparatus and Origin 7.0 (Lightstone Corp., Tokyo, Japan). The image plots were constructed from the second-derivative spectra by using SigmaPlot 10 (Systat Software Inc., USA).

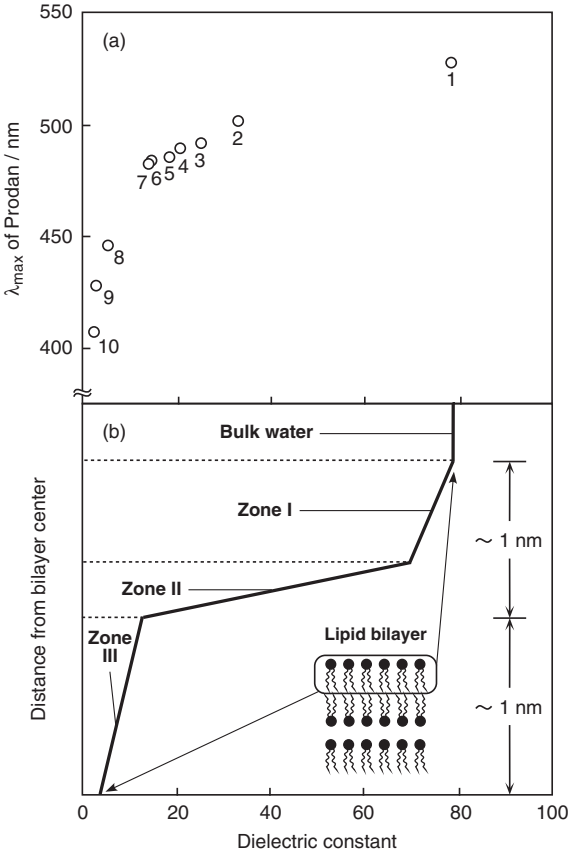

Figure 1. (a) Wavelength of fluorescence emission maximum for various solvents as a function of solvent dielectric constant at 25 °C and 0.1 MPa: (1) water, (2) methanol, (3) ethanol, (4) 1-propanol, (5) 1-butanol, (6) 1-pentanol, (7) 1-hexanol, (8) chloroform, (9) benzene, and (10) cyclohexane. (b) A schematic representation of the variation of the dielectric constant from the bilayer core to the bulk water. Three zones of lipid bilayer proposed by the zone model are drawn together with the size of the zones.

Results and Discussion

Location of Prodan in the PC Bilayer. When Prodan is dissolved in a solvent, its maximum emission wavelength (λ_{max}) is changed depending on the kinds of solvents. Figure 1a demonstrates the dependence of the λ_{max} values on the dielectric constant of a solvent at constant temperature and pressure. A good correlation between the λ_{max} value and the dielectric constant was observed. The higher λ_{max} value (e.g., 528 nm in water) corresponds to Prodan being in polar or hydrophilic environment whereas the lower value (e.g., 428 nm in benzene) does to Prodan being in less polar or hydrophobic environment.

On the other hand, when Prodan is incorporated into PC bilayers, the λ_{max} value is greatly dependent on the phase states of the bilayers: the value drastically varies at the phase transitions. Okamura and Nakahara have recently proposed a zone model for lipid bilayers.[24,25] In the model, the amphiphilic structure of phospholipids produces the gradient of dielectric constant in the bilayers, and hydrated lipid bilayers can be divided into three zones by the dielectric constant along the

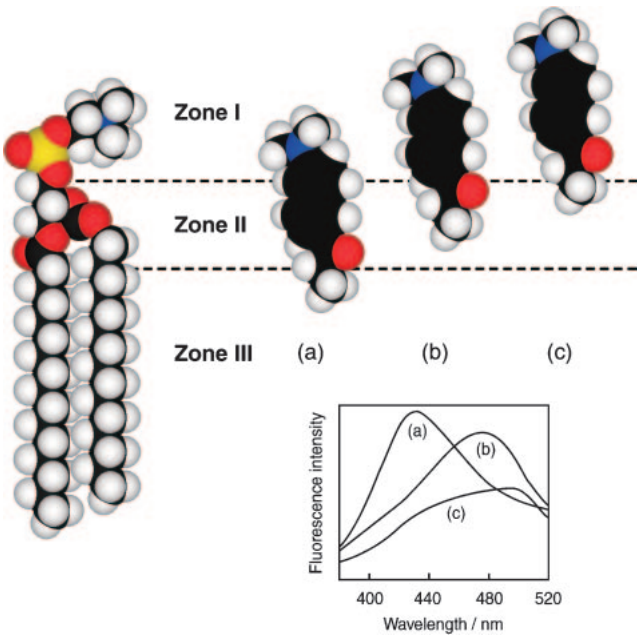

Figure 2. Schematic representation of Prodan location in different phases of the PC bilayer and the fluorescence behavior. Prodan molecules locate (a) around glycerol backbone (zone II) in the gel phase with a spectra of ca. 430 nm peak, (b) around phosphate (zones I and II) in the L_α phase with a spectra of ca. 480 nm peak, and (c) around lipid head group (zone I) in the $L_\beta I$ phase with a spectra of ca. 500 nm peak, respectively.

lipid molecule in the bilayer. Figure 1b schematically illustrates the proposed zone model and respective zone for the lipid molecule in the bilayer. Zone I is the hydrophilic part of bilayer with a high dielectric constant, and this region contains the polar head groups composed of choline and phosphate groups. Zone II is the interfacial region with a large gradient in the dielectric constant between the hydrophilic and the hydrophobic parts of the lipid, and this region contains the glycerol backbone and ester carbonyl group. Zone III is the hydrocarbon chain region with a low dielectric constant and consists of the bilayer core. We have found in previous studies[16,17] that the phases of gel, L_α, and one of nonbilayer phases, interdigitated gel ($L_\beta I$), for diacyl-PC bilayers show the λ_{max} values of about 430, 480, and 500 nm on the Prodan fluorescence spectra, respectively. The locations of the Prodan molecule in these phases were determined by comparing the λ_{max} values to these zones. The Prodan locations in the PC bilayer and representative spectrum for each phase are schematically drawn in Figure 2. The 430-nm peak in the gel phase indicates that the Prodan molecules exist in less polar region around glycerol backbone (zone II), the 480-nm peak in the L_α phase does that they exist in interface region between zones I and II such as the neighborhood of the phosphate group, and the 500-nm peak in the $L_\beta I$ phase does that they exist in hydrophilic region around lipid head group (zone I). The above fact suggests that the location of the Prodan molecules in the PC bilayer is closely related to the packing state in the respective phase, in other words, cross-sectional area of the PC molecules in the bilayer (0.41, 0.47, and 0.76 nm^2 for the gel, L_α and $L_\beta I$ phases).[26,27]

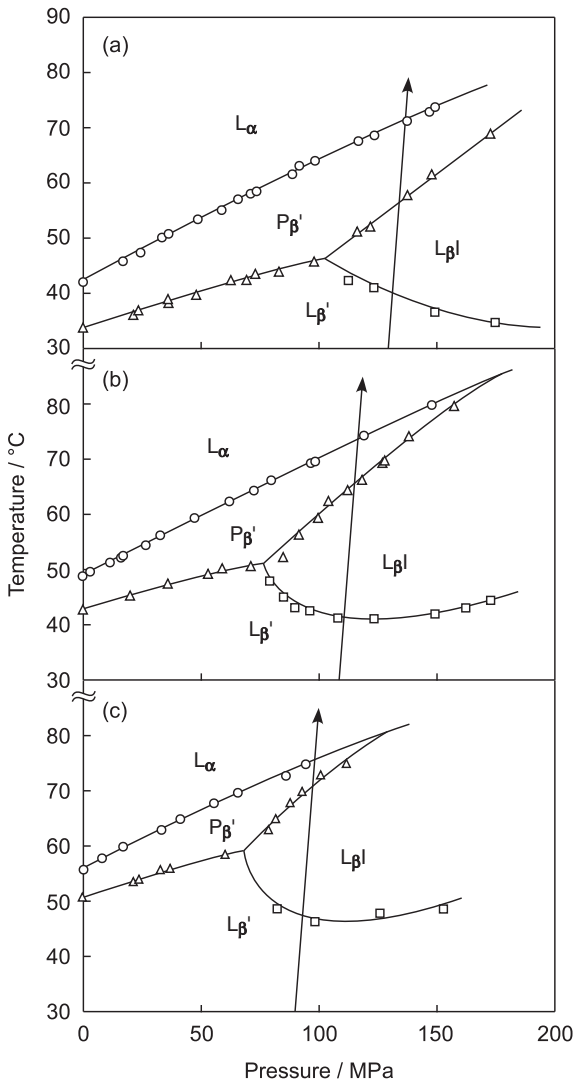

Figure 3. Temperature–pressure phase diagrams for C*n*PC bilayers: (a) C16PC, (b) C17PC, and (c) C18PC. An arrow in each diagram indicates the heating process for Prodan fluorescence measurements in Figures 4, 5, and 6.

Fluorescence Spectra of Prodan in the C16PC Bilayer. We have constructed the temperature (T) and pressure (p) phase diagrams of various kinds of PC bilayers.[14,15,20,21] Here we took up C16PC, known as dipalmitoyl-PC and abbreviated as DPPC. Since this lipid is one of the main constituents of membrane lipids in cell membranes, it is widely used in biophysical and biochemical research and regarded as a standard lipid in membrane studies. Figure 3a shows the T–p phase diagram of the C16PC bilayer. The C16PC bilayer undergoes two kinds of thermotropic phase transitions under atmospheric pressure, that is, the pretransition from the lamellar gel (L_β') phase to the ripple gel (P_β') phase at 34.3 °C and the main transition from the P_β' phase to the L_α phase at 42.0 °C in turn. Both transition temperatures increase linearly by applying pressure, and another gel phase, a pressure-induced $L_\beta I$ phase, appears between the L_β' and P_β' phases at pressures above about 100 MPa. The polymorphism of the gel phases (L_β', P_β', and $L_\beta I$) is a noticeable feature for the bilayers of PCs with a large and bulky choline head group.

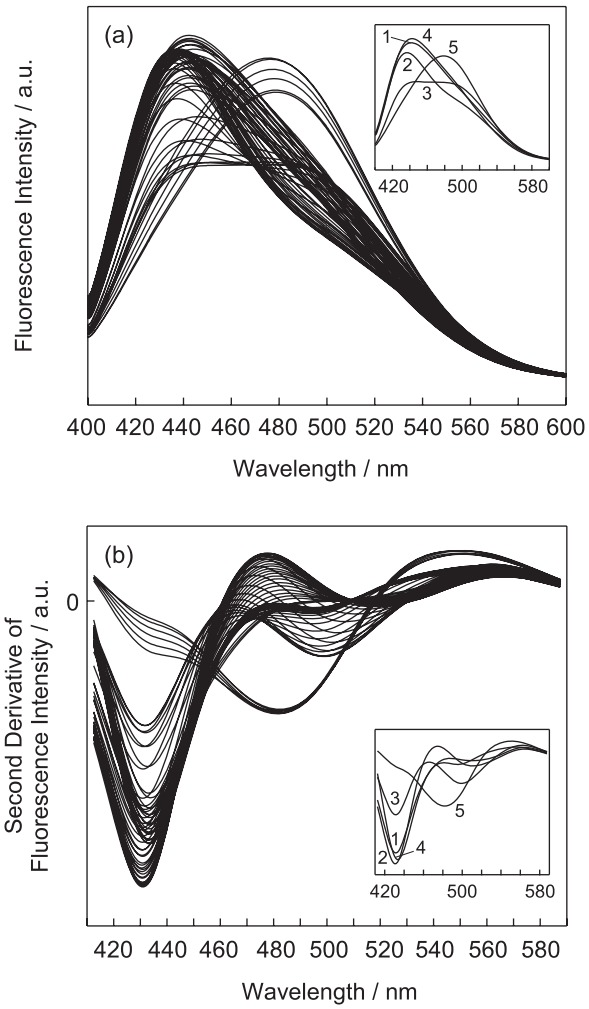

Figure 4. (a) Fluorescence spectra of Prodan in the C16PC bilayer at 128.4 MPa as a function of temperature. Here the spectrum is depicted every 1 °C from 19.5 and 78.2 °C. (b) The second-derivative spectra for the C16PC bilayer, which was constructed from the figure a. The inset in each figure shows the extraction of respective spectra at constant temperature: (1) 24.4, (2) 46.0, (3) 51.0, (4) 63.5, and (5) 78.2 °C.

By using the phase diagram of the C16PC bilayer, we measured the Prodan fluorescence on the bilayer with increasing temperature at constant pressure. Since the rigorous isobaric thermotropic process cannot be obtained because of a slight elevation of pressure by increasing temperature, we performed the experiments along the heating process indicated by an arrow in Figure 3a under high pressure. The resulting fluorescence spectra of the C16PC bilayer as a function of temperature are given in Figure 4a. The C16PC bilayer undergoes three kinds of phase transitions, the $L_{\beta'}/L_{\beta}I$, $L_{\beta}I/P_{\beta'}$, and $P_{\beta'}/L_{\alpha}$ transitions with an increase in temperature. We observed the characteristic spectral changes at the above phase transitions. Here the representative spectra at five temperatures, which were extracted from the original spectra, are shown as an upper inset in the figure. The λ_{max} value in the $L_{\beta'}$ phase at low temperatures around 25 °C (curve 1 in the inset in Figure 4a) was found to be 440 nm. The intensity at λ_{max} decreased with increasing temperature (curve 2). And then, in response to the appearance of the $L_{\beta}I$ phase, the spectra showed a 500-nm peak in addition to the 440-nm peak at around 50 °C (curve 3). Increasing temperature up to around 60 °C made the λ_{max} value go back to 442 nm on account of the $L_{\beta}I/P_{\beta'}$ transition (curve 4). Subsequently, the λ_{max} value increased again from 442 nm in the $P_{\beta'}$ phase to 480 nm in the L_{α} phase at the main transition of 73.5 °C (curve 5).

The second-derivative spectrum is often employed for a detailed analysis of spectrophotometric data.[28] When converting from an original emission spectrum to the second-derivative, major components as main peaks and minor components as small shoulder peaks in the original spectrum can be separated as clear individual peaks in the second-derivative spectrum although the λ_{max} in the original spectrum is also converted to the minimum wavelength (λ''_{mim}) in the second-derivative. We found that this peak separation is remarkably effective for an exact determination of the location of Prodan in the PC bilayer and used the second-derivative spectra of Prodan fluorescence to investigate the distribution and orientation behavior of Prodan in the PC bilayer.[20,21] The second-derivative spectra obtained from the original ones in Figure 4a are shown in Figure 4b. In the second-derivative spectra, at least four minima were seen: the λ''_{mim} values are 431, 434, 482, and 499 nm, respectively. It should be noted that the λ''_{mim} values are not always consistent with the λ_{max} values. This fact suggests that the original spectra consist of multiple components, indicating that the Prodan molecules can be distributed into multiple sites in the PC bilayer. One example of the existence of multiple sites is the distribution of Prodan in the $L_{\beta}I$ phase. When the second-derivative spectra exhibit 499-nm minima, the spectra contain relatively deep 431-nm minima simultaneously. This means that the Prodan molecules are distributed into the hydrophilic region as well as the glycerol backbone region in the $L_{\beta}I$ phase of the bilayer membrane. Because the λ''_{mim} appears in the order of 431, 499, 434, and 482 nm in turn in conformity with the phase sequence of $L_{\beta'}$, $L_{\beta}I$, $P_{\beta'}$, and L_{α} during the heating, we determined these wavelengths as the characteristic ones for four phases, respectively.

Imaging of Packing States in the C16PC Bilayer. A series of Prodan spectra were measured as a function of temperature, then it is possible to construct a three-dimensional image plot of the isobaric thermotropic change of the Prodan spectra shown in Figure 4 if the temperature intervals for a spectrum measurement are narrow and interpolated between consecutive temperatures. Since the movements of the Prodan molecules in the PC bilayer, that is, the change in their distribution and orientation in the bilayer are well correlated with the bilayer packing states, the plots provide the visual imaging of packing states in the PC bilayer.[22,23] The image plots of bilayer packing states for the C16PC bilayer were constructed by using data of original and second-derivatives spectra given in Figure 4. The resulting image plots for the original and second-derivatives spectra are depicted in Figures 5a and 5b, respectively. Here, the fluorescence intensity is drawn by a color scale as an indicator in the figures: the change from low intensity to high intensity is indicated by the

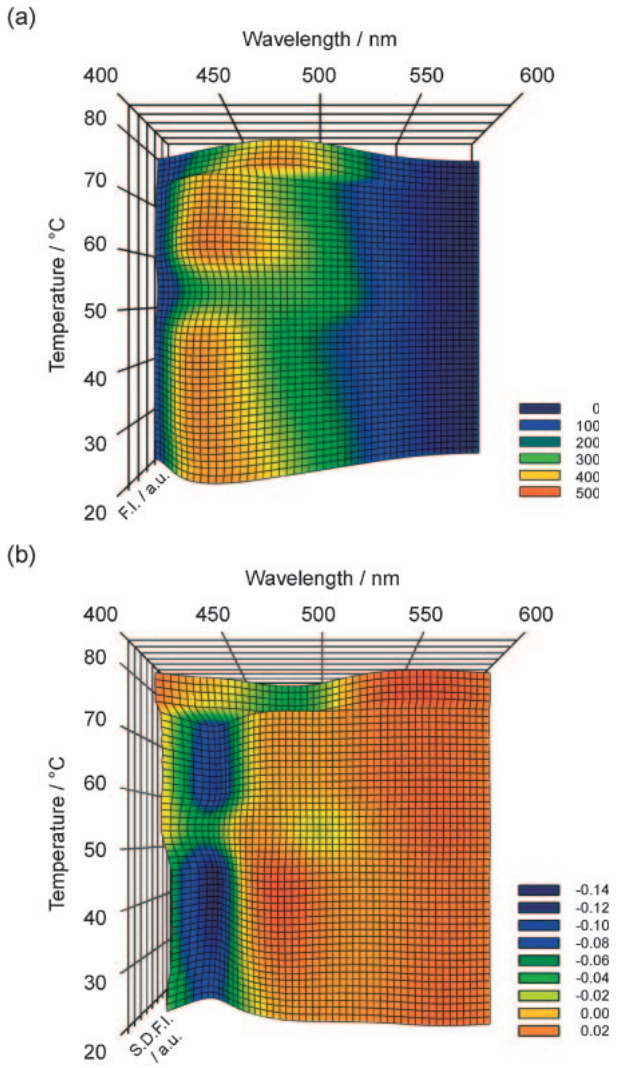

Figure 5. (a) Image plot for the fluorescence spectra of Prodan in the C16PC bilayer. (b) Image plot for the second derivatives of the fluorescence spectra of Prodan in the C16PC bilayer. Both plot were constructed from the spectra given in Figures 4a and 4b, respectively.

change of the color from blue to red in the order of the rainbow colors. We immediately noticed that the shape of contours in the image plot constructed from the original spectra is ambiguous as compared to that from the second-derivative spectra because the plot from the original spectra contains multiple components and they cannot be separated into respective components completely in the original spectra. Contrary to this, the plot from the second-derivative spectra can exhibit the change in the λ''_{mim} values much more sharply, which expresses the exact relationship between the fluorescence spectra and the bilayer phases. Accordingly, we adopted the latter plot as the visual imaging of packing states in the PC bilayer.

From the shape of contours in Figure 5b, the distribution and orientation of the Prodan molecules in the PC bilayer can be estimated from the depth of bluish valleys in the plot. We observed distinct five valleys in the plots, and the valleys correspond to the four phase states: two very deep bluish valleys at ca. 430 nm (the $L_{\beta'}$ phase (431 nm from 20 to 45 °C), the $P_{\beta'}$ phase (434 nm from 58 to 74 °C)), one deep greenish valley at ca. 480 nm (the L_{α} phase (482 nm from 74 to 80 °C)), and one shallow yellowish valley at ca. 500 nm (the $L_{\beta}I$ phase (499 nm from 45 to 58 °C)) with a greenish valley at ca. 430 nm. The valleys clearly changed at three temperatures corresponding to the $L_{\beta'}/L_{\beta}I$, $L_{\beta}I/P_{\beta'}$, and $P_{\beta'}/L_{\alpha}$ transition temperatures of the C16PC bilayer. Comparing the transition temperatures obtained from the interface region between these valleys in the plot to those determined from the *T*–*p* phase diagram in Figure 3a, the $L_{\beta}I/P_{\beta'}$ and $P_{\beta'}/L_{\alpha}$ transition temperatures were in agreement with each other, but the $L_{\beta'}/L_{\beta}I$ transition temperature in the plot was about 8 °C higher than that in the diagram. As shown in the Figure 4b, the second-derivative spectra of the $L_{\beta}I$ phase in the C16PC bilayer have two λ''_{mim} values of 431 and 499 nm, and the depth of the 431-nm minima are larger than that of the 499-nm minima. This is suggestive of the looser packing of the $L_{\beta}I$ phase of the C16PC bilayer. The higher temperature in the plot than in the diagram may be attributable to the localization of the Prodan molecules near the glycerol backbone region even in the $L_{\beta}I$ phase. It is understandable from the above behavior in the image plot of the second-derivative spectra that the bilayer packing states can be visualized only by one fluorescent probe Prodan.

Bilayer Packing of the PCs with Slight Different Acyl Chains. Let us now examine the packing behavior of other PC bilayers and compare it to that of the C16PC bilayer. It is interesting to see if the imaging technique can distinguish the bilayer packing states among PCs with a slight different hydrophobicity. We selected homologs of C16PC, C17PC, and C18PC, for this purpose. The *T*–*p* phase diagrams of the C17PC and C18PC bilayers are shown in Figures 3b and 3c, respectively. Although the phase behavior of these PC bilayers are similar to one another, all phase-transition temperatures are elevated with an increase in acyl chain length because of the enhancement of the acyl chain interaction between the PC molecules in the bilayer. A notable difference in phase behavior among these bilayers is the bilayer interdigitation. The pressure of a triple point among three gel ($L_{\beta'}$, $P_{\beta'}$, and $L_{\beta}I$) phases, which we call the minimum interdigitation pressure,[21] shifted to the lower pressure region with an increase in chain length.[14,21] The $L_{\beta}I$ phase is stabilized by the elongation of the acyl chain as well as the application of pressure.

We constructed the image plots of the C17PC and C18PC bilayers in a similar way. The image plots of both bilayers are drawn in Figure 6. Here the measurements of Prodan fluorescence for both bilayers were done along the heating process with the same phase sequence line under high pressure as the case of the C16PC bilayer. The image plots obtained for both bilayers produced a pronounced difference compared to that of the C16PC bilayer inspite of the same phase sequence on the phase diagrams. The valleys observed in the C16PC bilayer were completely separated into four valleys in the C17PC bilayer. Therefore, we can say that the location of Prodan in the PC bilayer is firmly immobilized in each phase of the C17PC bilayer. In the C18PC bilayer, the valley at ca. 430 nm and ca. 70 °C, which originates from the $P_{\beta'}$ phase, nearly disappeared.

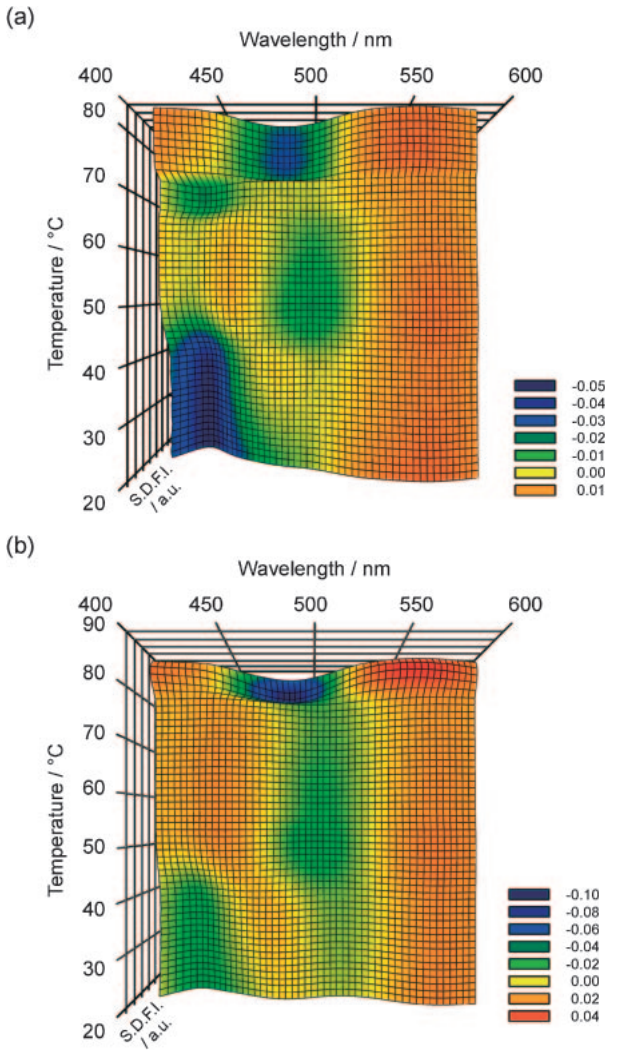

Figure 6. Image plots for the second derivatives of fluorescence spectra of Prodan in the PC bilayers: (a) C17PC at 105.6 MPa in the temperature range of 20.0–84.5 °C, (b) C18PC at 85.3 MPa in the temperature range of 19.5–83.0 °C.

We compared the distribution behavior of the Prodan molecules in the respective phase among the three PC bilayers. The bluish valleys for the bilayer gel, $L_{\beta'}$ and $P_{\beta'}$ phase at ca. 430 nm became shallower with an increase in acyl chain length, whereas the valley for the L_α phase at ca. 480 nm conversely became deeper with the acyl chain length. This contrasting change of the bilayer gel and L_α phases implies that the quantity of the Prodan molecules distributed into the glycerol backbone region decreases while that into phosphate region increases with the chain elongation. That is, the Prodan molecules preferentially locate the glycerol backbone region in the C16PC bilayer while they preferentially do the phosphate region in the C18PC bilayer. Since the cohesive force among the PC molecules in their bilayers becomes stronger with an increase in acyl chain length, the bilayer packing becomes tighter with the acyl chain length. Then, the relative ease with which the Prodan molecules partition to the glycerol backbone is inversely proportional to the hydrophobicity of the PC molecules, and the situation becomes vice versa in the L_α phases. Regarding the distribution in the nonbilayer gel, L_βI phase, the yellowish valley observed in the C16PC bilayer changed the greenish valleys in the C17PC and C18PC bilayers, which means that greater numbers of Prodan molecules partition into the hydrophilic region around lipid head group in the C17PC and C18PC bilayers in comparison with the C16PC bilayer. Taking into account that the C16PC bilayer has a shallow yellowish valley at ca. 500 nm and a greenish valley at ca. 430 nm simultaneously and the $L_{\beta'}/L_\beta$I transition apparently occurs at a temperature higher than ca. 8 °C, this indicates that the enhanced packing of the L_βI phases of the C17PC and C18PC bilayers excludes the Prodan molecules in the glycerol backbone to the hydrophilic region entirely.

Furthermore, in the case of the C18PC bilayer, another shallow light-greenish valley at ca. 515 nm and below 40 °C appeared together with the greenish valley at ca. 430 nm. With increasing temperature, the two valleys incorporated into one greenish valley of the L_βI phase at ca. 500 nm. The 515-nm valley implies that the Prodan molecules reside in the most hydrophilic region at the bilayer surface taking into account that the λ_{max} value of Prodan in water is 528 nm as given in Figure 1a. The cohesive force of the C18PC molecules in the bilayer is the strongest among the present PC molecules, and the bilayer packing in the gel phase becomes the tightest. This valley is attributed to the fact that a part of the Prodan molecules are squeezed out from the head-group region due to the tight packing. We have also observed the similar exclusion of the Prodan molecule in a system of giant multilamellar vesicles with dense and tight packing.[22] The exclusion of the Prodan molecules in the bilayer gel phase offers an obvious proof of a rigid packing of the bilayers.

Conclusion

The packing states of the C16PC bilayer were evaluated from the distribution and orientation behavior of a polarity sensitive probe Prodan incorporated into the bilayer by means of a high-pressure fluorescence technique. We constructed the image plot on the basis of the second-derivative spectra of the Prodan fluorescence and could visually reveal that the Prodan molecules can move around the head-group region sensitively responding to the phase state of the bilayer. Further, it was proven that the difference in the packing state among the C16PC, C17PC, and C18PC bilayers, which caused by the slight change in hydrophobicity among the molecules, can be sensitively captured in the image plots. The imaging by using a good packing indicator Prodan enables us to study the bilayer packing of lipids in detail.

References

1 A. Seelig, J. Seelig, *Biochemistry* **1974**, *13*, 4839.
2 M. R. Morrow, J. P. Whitehead, D. Lu, *Biophys. J.* **1992**, *63*, 18.
3 X. Peng, A. Jonas, J. Jonas, *Biophys. J.* **1995**, *68*, 1137.
4 H. M. McConnell, W. L. Hubbell, *J. Am. Chem. Soc.* **1971**, *93*, 314.
5 E. J. Shimshick, H. M. McConnell, *Biochemistry* **1973**, *12*, 2351.

6 J. R. Trudell, D. G. Payan, J. H. Chin, E. N. Cohen, *Biochim. Biophys. Acta, Biomembr.* **1974**, *373*, 436.
7 K. Ruan, R. Lange, Y. Zhou, C. Balny, *Biochem. Biophys. Res. Commun.* **1998**, *249*, 844.
8 H.-J. Galla, W. Hartmann, *Chem. Phys. Lipids* **1980**, *27*, 199.
9 J. Zeng, P. L. Chong, *Biophys. J.* **1995**, *68*, 567.
10 T. Parasassi, G. De Stasio, A. d'Ubaldo, E. Gratton, *Biophys. J.* **1990**, *57*, 1179.
11 T. Parasassi, G. De Stasio, G. Ravagnan, R. M. Rusch, E. Gratton, *Biophys. J.* **1991**, *60*, 179.
12 F. M. Harris, K. B. Best, J. D. Bell, *Biochim. Biophys. Acta, Biomembr.* **2002**, *1565*, 123.
13 L. A. Bagatolli, *Biochim. Biophys. Acta, Biomembr.* **2006**, *1758*, 1541.
14 H. Ichimori, T. Hata, H. Matsuki, S. Kaneshina, *Biochim. Biophys. Acta, Biomembr.* **1998**, *1414*, 165.
15 H. Matsuki, E. Miyazaki, F. Sakano, N. Tamai, S. Kaneshina, *Biochim. Biophys. Acta, Biomembr.* **2007**, *1768*, 479.
16 M. Kusube, H. Matsuki, S. Kaneshina, *Colloids Surf., B* **2005**, *42*, 79.
17 M. Kusube, N. Tamai, H. Matsuki, S. Kaneshina, *Biophys. Chem.* **2005**, *117*, 199.
18 P. L.-G. Chong, *Biochemistry* **1988**, *27*, 399.
19 J. Zeng, P. L.-G. Chong, *Biochemistry* **1991**, *30*, 9485.
20 M. Goto, M. Kusube, N. Tamai, H. Matsuki, S. Kaneshina, *Biochim. Biophys. Acta, Biomembr.* **2008**, *1778*, 1067.
21 M. Goto, S. Ishida, N. Tamai, H. Matsuki, S. Kaneshina, *Chem. Phys. Lipids* **2009**, *161*, 65.
22 M. Goto, H. Sawaguchi, N. Tamai, H. Matsuki, S. Kaneshina, *Langmuir* **2010**, *26*, 13377.
23 M. Goto, T. Matsui, N. Tamai, H. Matsuki, S. Kaneshina, *Colloids Surf., B* **2011**, *84*, 55.
24 E. Okamura, M. Nakahara, in *Liquid Interfaces in Chemical, Biological, and Pharmaceutical Applications*, ed. by A. G. Volkov, Marcel Dekker, New York, **2000**, pp. 775–805.
25 E. Okamura, M. Nakahara, *Int. Congr. Ser.* **2005**, *1283*, 203.
26 M. J. Ruocco, G. G. Shipley, *Biochim. Biophys. Acta, Biomembr.* **1982**, *691*, 309.
27 P. Laggner, K. Lohner, G. Degovics, K. Müller, A. Schuster, *Chem. Phys. Lipids* **1987**, *44*, 31.
28 T. Ichikawa, H. Terada, *Biochim. Biophys. Acta, Protein Struct.* **1977**, *494*, 267.